High-efficiency Bragg gratings in photothermorefractive glass

Oleg M. Efimov, Leonid B. Glebov, Larissa N. Glebova, Kathleen C. Richardson, and Vadim I. Smirnov

Photosensitive silicate glasses doped with silver, cerium, fluorine, and bromine were fabricated at the Center for Research and Education in Optics and Lasers. Bragg diffractive gratings were recorded in the volume of these glasses with a photothermorefractive process (exposure to UV radiation of a He–Cd laser at 325 nm is followed by thermal development at 520 °C). Absolute diffraction efficiency of as much as 93% was observed for 1-mm-thick gratings with spatial frequencies up to 2500 mm^{-1}. No decreasing of diffraction efficiency was detected at low spatial frequencies. Original glasses were transparent (absorption coefficient less than 1 cm^{-1}) from 350 to 4100 nm. Induced losses in exposed and developed glass decreased from 0.3 to 0.03 cm^{-1} between 400 and 700 nm, respectively, and did not exceed 0.01–0.02 cm^{-1} in the IR region from 700 to 2500 nm. Additional losses caused by parasitic structures recorded in the photosensitive medium were studied. © 1999 Optical Society of America

OCIS codes: 050.7330, 090.2900, 160.2750.

1. Introduction

Increasing applications for holographic optical elements have resulted in continued development of new effective and reliable photosensitive media. The recent Hariharan book[1] notes that the main photosensitive materials available for high-efficiency hologram recording are silver halide photographic emulsions, dichromated gelatin, photoresists, photopolymers, photothermoplastics, polymers with spectral hole burning, and photorefractive crystals. Each of these materials has their merits, but all have drawbacks. Organic materials (photographic emulsions, dichromated gelatin, and photopolymers) are sensitive to humidity. Moreover, they significantly shrink in the development process. Inorganic materials (photorefractive crystals) have low resistance to elevated temperatures and produce additional patterns because of exposure to the beam diffracted from the recorded grating. "The ideal recording material for holography should have a spectral sensitivity well matched to available laser wavelengths, a linear transfer characteristic, high resolution, and low noise, be indefinitely recyclable or relatively inexpensive. While several materials have been studied, none has been found so far that meets all these requirements."[1] The lack of available materials for phase holography stimulates the search for new approaches. In this paper we describe properties and performance of a new inorganic glass as a medium for hologram recording, which meets practically all the requirements indicated above.

Use of inorganic photosensitive glasses for phase hologram recording was described several years ago in Refs. 2–4. Bragg gratings were recorded in lithium aluminum silicate[2] and sodium zinc aluminum silicate[3,4] glasses doped with silver and cerium by exposure to UV radiation followed by thermal treatment. This phenomenon was named the photothermorefractive (PTR) process. Glasses, which possess such properties, were called photothermorefractive glasses.

The photothermal process based on precipitation of dielectric microcrystals in the bulk of glass exposed to UV radiation was discovered by Stookey in 1949.[5] This two-step process (exposure and thermal development) was used to record a translucent image in glass because of light scattering caused by a difference between the refractive indices of a precipitated crystalline phase and the glass matrix. Later, colored images were recorded in similar glasses by photothermal precipitation of a number of complex

The authors are with the Center for Research and Education in Optics and Lasers, University of Central Florida, Orlando, Florida 32816-2700.

Received 31 August 1998; revised manuscript received 9 November 1998.

0003-6935/99/040619-09$15.00/0

crystals of different compositions, sizes, and shapes.[6–8] The link of processes, which occur in these glasses and produce coloration, was described in Refs. 5 and 6. According to these studies, the first step is the exposure of the glass sample to UV radiation, which produces ionization of a cerium ion. The electrons released from cerium are then trapped by a silver ion. As a result, silver is converted from a positive ion to a neutral atom. This stage corresponds to a latent image formation, and no significant coloration occurs.

The next step is a thermal development, which is a process that includes two stages. The first stage involves the high diffusion rate that silver atoms possess in silicate glasses. This diffusion leads to the creation of tiny silver crystals at relatively low temperatures (450–500 °C). A number of silver clusters arise in exposed regions of glass after aging at elevated temperatures. These silver particles serve as the nucleation centers for sodium and fluorine ion precipitation, and cubic sodium fluoride crystal growth occurs at temperatures between 500 and 550 °C. Further heat treatment leads to the growth of elongated pyramidal complex Na,Ag-F,Br crystals on the surface of cubic NaF crystals. This mixture of crystals can produce opal coloration in the case of large crystal sizes or yellow coloration caused by colloidal silver precipitated on interfaces of dielectric crystals. A second exposure to UV followed by a second heat treatment produces different coloration because of metallic silver reduction on the surfaces of the dielectric pyramids. The final resulting coloration depends on the size and aspect ratio of these silver particles. This multistage photothermal process in photosensitive glass was proposed for decoration, color photography, sculpture, and even for holography. However, no difference of refractive indices of exposed and unexposed sites was found at that time, and the first phase holograms were recorded in photosensitive glasses many years later.[2,3]

It was found in Refs. 3 and 4, which describe dielectric crystal precipitation in glasses exposed to radiation of the nitrogen laser at 337 nm, that a refractive-index decrease of approximately 5×10^{-4} occurs. The refractive index of NaF in the red spectral region is $n_{\mathrm{NaF}} = 1.32$ in comparison with the refractive index of PTR glass $n_{\mathrm{PTR}} = 1.49$ (Ref. 4). The small value of refractive-index change is due to the small volume fraction of the precipitated crystalline phase. However, it is sufficient enough to result in a high-efficiency Bragg grating recording in samples with thicknesses more than several hundreds of micrometers. Conditions of glass exposure and development were found in that research to create Bragg gratings with relative diffraction efficiency up to 90% and angular selectivity up to 2 mrad. The maximum recorded spatial frequency was 2500 mm^{-1}. These gratings were stable up to 400 °C. The photosensitivity was found in the range of several joules per square centimeter at a nitrogen laser wavelength (337 nm). The absorption band of Ce^{3+}, which is used for photoionization, has a maximum near 300 nm and a long wavelength tail up to 400 nm. This means that several commercial lasers such as N_2, Ar, He–Cd, etc. can be used for recording. Once developed, holograms in PTR glass were not destroyed by further exposure to visible light. The price of this photosensitive silicate glass is rather small in comparison with other photosensitive materials. Unfortunately, this new material has not met all requirements formulated in Ref. 1 because of strong scattering, which arises in the process of development. This scattering resulted in low absolute diffraction efficiency of gratings in PTR glasses, which did not exceed 45%. Thus a new and promising material for holographic optical elements, which was announced in Refs. 3 and 4, was not free of all drawbacks.

The goal of this research was to find if high losses are an intrinsic feature of PTR glass or if, with the proper choice of glass technology and conditions of exposure and thermal development, this phenomenon can be eliminated. To do this we developed a laboratory technology of PTR glass melting and samples preparation; studied absorption spectra of original, exposed, and developed PTR glasses in the UV, visible, and IR regions; and studied Bragg grating optical properties versus conditions of UV exposure and thermal treatment. Different types of losses, which appeared in the process of hologram recording, were studied, and requirements for sample preparation and recording procedure were formulated.

2. Experiment

The same photosensitive glass of approximate composition (mol.%) $15Na_2O$-$5ZnO$-$4Al_2O_3$-$70SiO_2$-$5NaF$-$1KBr$-$0.01Ag_2O$-$0.01CeO_2$ was studied in this research as in previous research.[3,4] The glass was melted in an electrical furnace (DelTech Model DT-31-RS-OS) in 400-ml fused-silica crucibles at 1460 °C for 5 h. Stirring was used to homogenize the melt. After the melting, the glass was poured onto a thick metal slab to avoid spontaneous crystallization. The glass casting underwent annealing with a cooling rate in the region of structural and stress relaxation of 0.2 °C/min in a Lindberg/BlueM box furnace. Thermal development was produced by keeping the exposed specimen in the same furnace at a temperature of 520 °C from periods of a few of minutes to several hours. Polished glass samples from 0.5- to 10-mm thickness of 12 mm × 25 mm in size were prepared with a Buehler Ecomet-3 grinder/polisher with an Automet-2 power head. Optical homogeneity of samples was tested by the shadow method in the divergent beam of a He–Ne laser.

Absorption spectra from 200 to 5000 nm were measured with a double-beam Perkin-Elmer 330 and a single-beam Perkin-Elmer 1600 Fourier-transform infrared spectrophotometers. To avoid uncertainty in the absorption coefficient caused by dispersion of surface losses in such a wide spectral area, optical densities (D_1 and D_2) for two samples of different thicknesses (l_1 and l_2) were measured for each glass.

The absorption coefficient was calculated as $A = D_1 - D_2/l_1 - l_2$. Absorption spectra measured by UV to visual and IR spectrophotometers were merged at 2300 nm because of the lowest glass absorption value in the spectral region of overlap between the short- and long-wavelength spectrophotometers. Additional absorption induced by exposure to UV radiation and heat treatment (A_{ad}) was calculated as $A_{ad} = A_{ex} - A$, where A_{ex} and A are absorption coefficients of the exposed and original specimens. Actually it is necessary to take into account a distribution of induced absorption along the beam propagation in the sample that is caused by a decreasing of exciting beam intensity. We used the averaged data, as shown above, because glass absorption at the wavelength of exposure (325 nm) is too low ($\sim$0.5 cm^{-1}). This caused attenuation of no more than 10% in a 1-mm-thick sample that was usually used for experiments and allowed us to use these data for loss evaluation. Total accuracy of the absorption coefficient measurement was ± 0.01 cm^{-1}.

Glasses were exposed to radiation of a single transverse-mode 1-mW He–Cd laser (Kimmon Electric Model RM3021R-L) at 325 nm. The laser beam passed through a telescope with variable expansion from 1^x to 10^x and a spatial filter. Exposure to a homogeneous single beam was used for the induced absorption spectra, the optical microscopy, and the light-scattering study. Periodic motion of the sample holder for approximately 0.5 mm in the direction perpendicular to the direction of the exciting beam was used in the exposure process to distinguish phenomena caused by imperfections of the laser beam or specimen. An exposure to the interference pattern was used to produce Bragg gratings in glass. To do this, the beam was split and then matched under different angles, which secured spatial frequencies in the glass sample from 250 to 2500 mm^{-1}. Holographic gratings of approximately 5 mm $\times$ 5 mm in size were recorded in samples ranging in thickness up to 2 mm.

The features of the recorded patterns were observed in the samples, which were polished on all sides, using an optical microscope. This approach allowed the recording of patterns from different directions. A single transverse-mode He–Ne laser at 633 nm was used for the study of photothermo-induced phenomena in PTR glass. Patterns of the scattered light of the He–Ne laser from a glass sample produced by UV exposure and thermodevelopment were recorded with a CCD camera (Sony XC-77). The dependencies of these patterns on conditions of recording (single and dual beams) and reading (different deviation from the Bragg angle) were explored. The diffraction patterns were studied for Bragg gratings recorded in PTR glasses. Intensities of incident beam (I_L), transmitted beam (I_0), and diffracted beam (I_1) were measured by a two-head power meter (Ophir Laser Star). The reflection coefficient (ρ) was calculated by the Fresnel formula[9] $\rho = (n - 1/n + 1)^2$. Relative and absolute diffraction efficiencies were calculated as

$$\eta_R = \frac{I_1}{I_0 + I_1}, \tag{1}$$

$$\eta_A = \frac{I_1}{(1 - \rho)^2 I_L}. \tag{2}$$

We used a term that was responsible for reflection in the formula for the absolute diffraction efficiency [Eq. (2)] to obtain data connected with the losses in the recording medium because reflection losses can be eliminated easily with an antireflection coating. The relative diffraction efficiency [Eq. (1)] allows a description of the oscillating part of the induced refractive index by Kogelnik's formula[1]:

$$\delta n = \frac{\lambda \cos \Theta \arcsin(\sqrt{\eta_R})}{\pi d}, \tag{3}$$

where λ is the wavelength of the reading beam, Θ is the Bragg angle, and d is the thickness of the specimen.

3. Results and Discussion

A. Absorption Spectra

Absorption spectra of PTR glasses are presented in Fig. 1. Figure 1(a) shows the UV part of the absorption spectrum. One can see the wide absorption band of Ce^{3+} (Refs. 5 and 8) with a maximum at 305 nm. The short-wavelength absorption in the region $\lambda < 270$ nm is due to a number of glass components, such as Ce^{4+}, Ag^+, Br^-, Fe^{3+}, and others. The exact analysis of this part of the absorption spectrum is a separate, complex problem and should be considered in other research. From the point of view of technical application, the short-wavelength edge, at which the writing radiation is attenuated by two times in the recording medium (optical density approximately 0.3), is placed at 330 nm for a 1-cm-thick plate and at 265 nm for 1-mm-thick plate. The range of photosensitivity of this glass in accordance with Refs. 3–5 is from 280 to 360 nm.

Absorption of PTR glass is less than 0.01 cm^{-1} in the visible and near-IR regions, and therefore it is not shown in Fig. 1. One can see in Fig. 1(b) detectable absorption at wavelengths more than 2700 nm. Absorption in this spectral region is usually ascribed to different vibrations of hydroxyl groups in the glass network[10] and reaches several inverse centimeters in silicate glasses. Hydroxyl absorption in fluorine containing PTR glass is lower compared with similar fluorine-free silicate glass. We believe that this phenomenon is caused by high volatilization of HF molecules, which can be produced as a result of interaction of fluorine and hydrogen in the process of glass melting. From a technical point of view, this decrease of the IR absorption in PTR glass results in an opportunity for PTR use in the middle IR region up to 4300 nm for a 1-mm-thick specimen. Hence

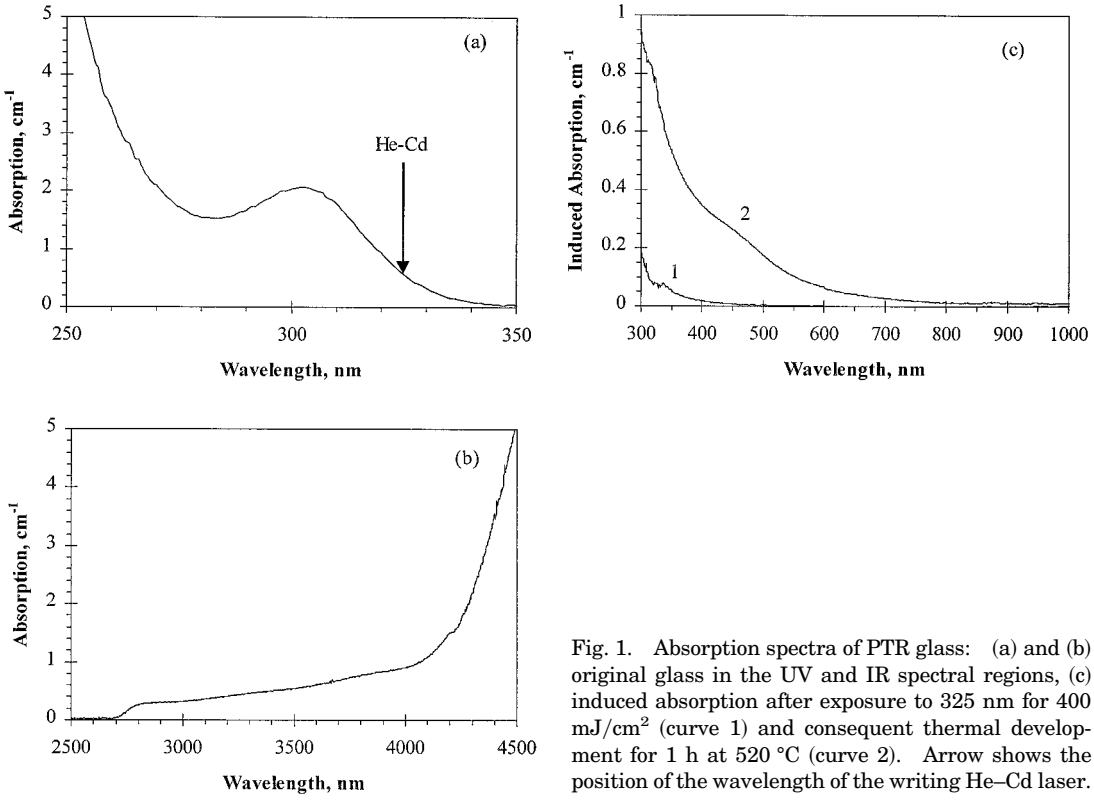

Fig. 1. Absorption spectra of PTR glass: (a) and (b) original glass in the UV and IR spectral regions, (c) induced absorption after exposure to 325 nm for 400 mJ/cm^2 (curve 1) and consequent thermal development for 1 h at 520 °C (curve 2). Arrow shows the position of the wavelength of the writing He–Cd laser.

Figs. 1(a) and 1(b) show that PTR glass is more transparent than usual optical crown glass and can be used in the near-UV, visible, and IR regions up to 4000 nm.

An additional absorption of PTR glass undergoing UV exposure, used in hologram recording in this glass, is shown in Fig. 1(c), curve 1. Detectable photoinduced absorption is seen only in the UV region. Even at the recording wavelength, this absorption is less 0.1 cm^{-1} and cannot impact the recording process significantly. The small tail of the induced absorption spectrum in the blue region can be distinguished by the naked eye as a slight yellow coloration of the exposed area. Thermodevelopment causes colloidal silver and sodium fluoride precipitation in the glass matrix.[5,6] Fluoride crystals are colorless and can result in scattering if the size of the crystals is too large (more than 100 nm). A shoulder near 450 nm in the additional absorption spectrum after thermal treatment in Fig. 1(c) (curve 2) was ascribed to silver particles in the glass matrix.[6] One can see that the visible additional absorption does not exceed 0.3 and 0.03 cm^{-1} in the blue and red regions, respectively. This means that losses in this region do not exceed a few percent for a 1-mm-thick plate. Additional absorption in the entire IR region is not detectable and therefore is not shown in Fig. 1(c). Consequently, this glass can be used successfully at all wavelengths in the visible and near-IR regions important for lasers and optical communication. It was found in Refs. 3 and 4 that absorption and scattering losses in specimens sufficiently exposed for high diffraction efficiency of Bragg gratings have exceeded 50%. We show in Subsection 3.D that conditions of exposure and thermal development for PTR glasses studied in this research resulted in additional absorption of hundredths of inverse centimeters [Fig. 1(c)]. This corresponds to almost 100% relative diffraction efficiency at 633 nm in a 1.5-mm-thick sample and more than 90% absolute diffraction efficiency.

B. Parasitic Phase Structures

Optical microscopy of exposed and developed samples used for induced absorption measurements has shown optical inhomogeneities in the exposed region. The structure of these inhomogeneities appears as a series of parallel, continuous, aligned filaments having widths of tens of micrometers oriented along the direction of light propagation in the glass sample. These microscopic features can be caused by structures with different refractive indices arising in the glass processing (phase structures). A similar fiberlike structure has been described in the photosensitive organic glass [poly(methyl methacrylate)] after Bragg grating recording.[11] No further experiments were made to clarify the nature of the phenomenon at this time.

One can suppose that these phase structures can be intrinsic features of these particular materials or caused by various imperfections in the optical system and recording medium, in spite of the homogeneity of the glass and the high quality of the beam after spa-

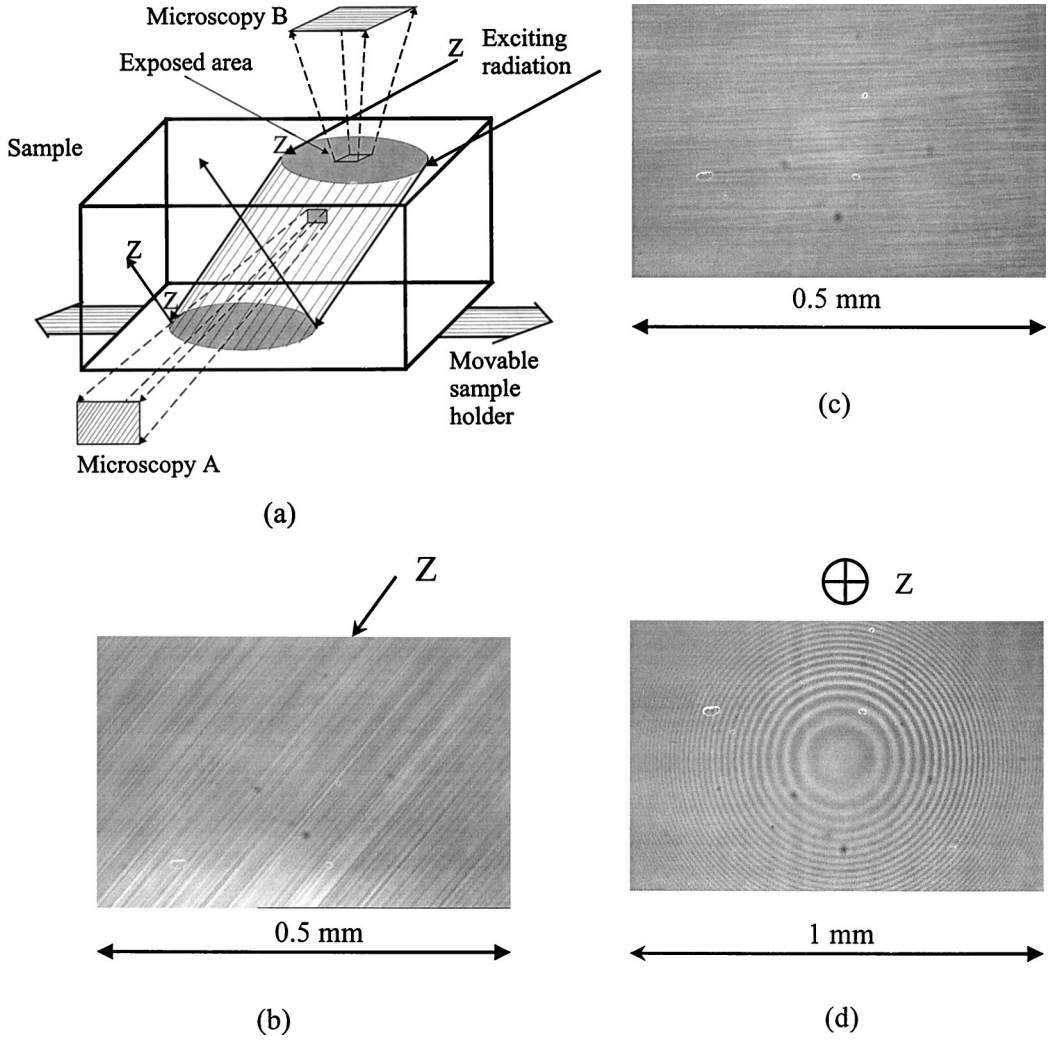

Fig. 2. Parasitic phase structures recorded in glass. (a) Experimental setup. Exciting radiation of the He–Cd laser at 325 nm was launched at the top surface of the specimen to produce a cylindrically exposed area in the glass bulk. No interference with reflected beams occurs in the top part of exposed area. Optical microscopy from the polished front side of the sample (A) and from the topside (B) was accomplished. Arrows show the directions of displacements of the movable sample holder. (b) Optical micrograph of the rain-type structure from position A. (c) Optical micrograph of the rain-type structure from position B. (d) Optical micrograph of the ring-type structure from position B.

tial filtering. To study this phenomenon, the experimental setup shown in Fig. 2(a) was used. The exciting laser beam diameter, angle of incidence, and a specimen thickness were chosen to avoid overlapping between propagating and back surface reflecting beams in the studied volume. Typical micrographs of the exposed region of the sample with multiple surface defects made from different positions [Fig. 2(a) are shown in Figs. 2(b) and 2(c). In Fig. 2(b) the filaments are directed along the beam propagation direction Z [shot from position A in Fig. 2(a)]. Figure 2(c) shows a view of this pattern from the front surface of the sample [position B in Fig. 2(a)]. Analysis of these and similar pictures shows that the visible microscopic filaments are not a system of strictly parallel lines. These filaments are elongated in the direction of light propagation and usually have a length no more than 1 or 2 mm. Actually they appear not only at the surface but at all distances of the beam propagation. The filaments are oriented mainly in the direction of the beam propagation but are not strictly parallel.

To select effects caused by beam and sample features, we produced several consequent motions of the sample holder during the exposure process, as shown in Fig. 2(a). In this case, all imperfections of the laser beam should be averaged and do not contribute to the recorded pattern. It was found that the spatial frequency of the quasi-periodical structure decreased in the movable sample. It was possible to distinguish individual diffractive patterns produced by surface pits, scratches, and volume inclusions (bubbles or stones). An exposed area in a perfect (free of visible microscopic surface and volume defects) movable sample was found to be completely homogeneous. This result allows us to conclude that

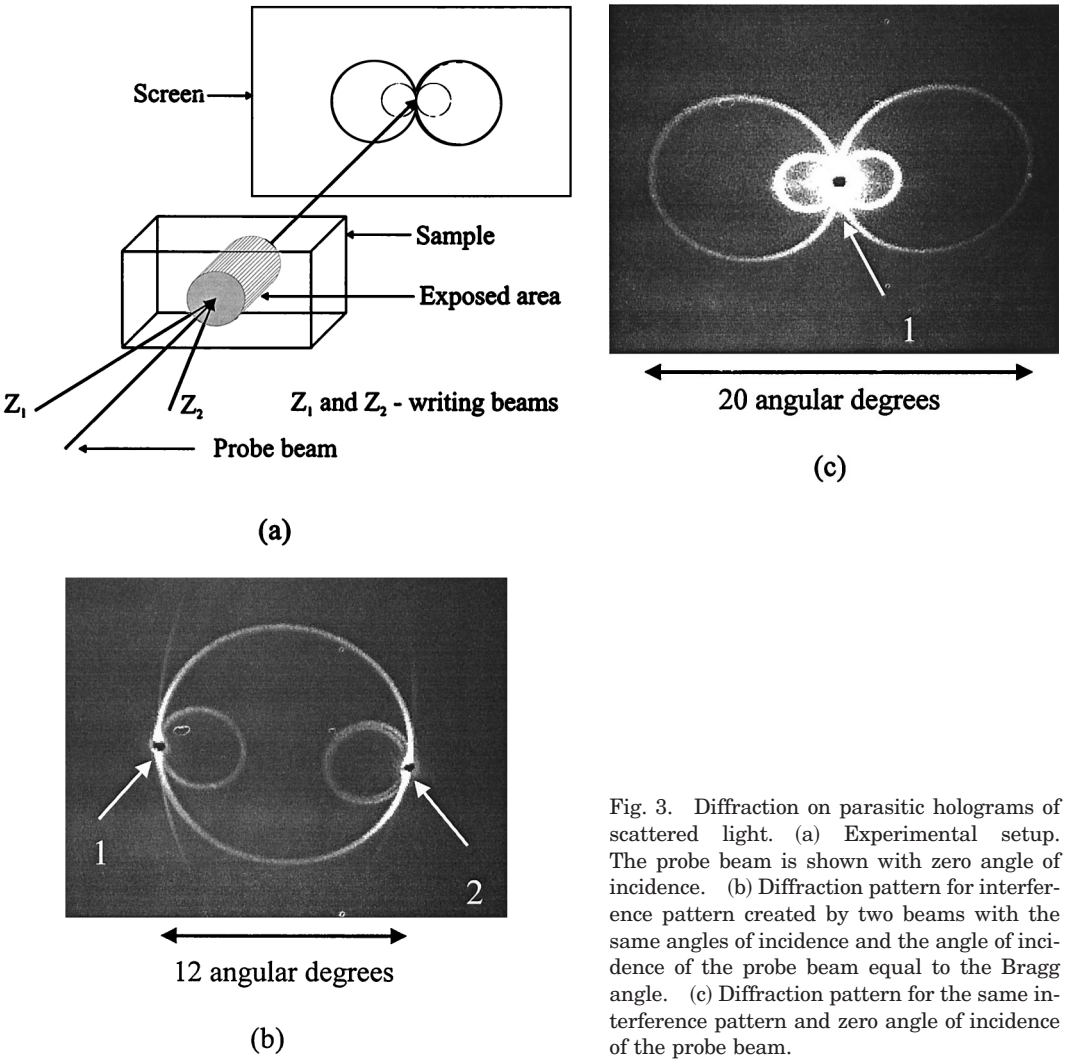

Fig. 3. Diffraction on parasitic holograms of scattered light. (a) Experimental setup. The probe beam is shown with zero angle of incidence. (b) Diffraction pattern for interference pattern created by two beams with the same angles of incidence and the angle of incidence of the probe beam equal to the Bragg angle. (c) Diffraction pattern for the same interference pattern and zero angle of incidence of the probe beam.

studied phase patterns are not an intrinsic feature of PTR glass but can be caused by various defects of glass and sample surfaces.

However, some additional patterns were found in micrographs made from position B in Fig. 2(a) in a motionless specimen. These patterns were combinations of different rings and fringes. It was found that this is a recording of an interference pattern produced by matching the propagating beam with the beam consequently reflected from the back and front surfaces of different elements in the optical setup. As an example, an interference pattern is shown in Fig. 2(d), which is produced by double reflection from the last lens of the spatial filter. Double reflection from plane elements (filters, etc.) gives a system of periodical straight fringes. Diffraction of the exciting beam on different apertures produces systems of straight or curved fringes with a variable period in dependence on the shape and position of the aperture. It is necessary to produce special adjustment to eliminate these interference and diffraction patterns in the plane of recording to avoid these parasitic structures. Therefore homogeneity of the photosensitive medium (including surface and volume defects) and the writing beam (including interference and diffraction patterns of low visibility) are to be tested to avoid undesirable losses.

C. Parasitic Hologram of Scattered Ultraviolet Radiation

The examination of exposed and developed specimens as shown in Fig. 3(a) was performed with a He–Ne laser probe beam for different angles of incidence. It was found that the pattern of the probe radiation transmitted through the exposed area consists not only of the zero and first orders of diffraction but exhibit some rings. The diameter and position of these rings on the screen [Fig. 3(a)] depends on the incidence angle of the probe beam and on the feature of the writing pattern. The case in which an interference pattern was recorded by two writing beams with the same angles of incidence and the incidence angle of a probe beam coincident with the Bragg angle is shown in Fig. 3(b). One can see in this figure two small rings next to the diffracted and transmitted beams, a large ring connecting these beams, and initial parts of two great rings, which cannot be placed

as a whole in this photo. The case with the same interference pattern but with zero incidence angle of the probe beam is shown in Fig. 3(c). In this figure one can see two small rings and two large rings, which gather at the position of the transmitted beam. Deviation from the normal incidence leads to elimination of symmetry between the left and right rings. Use of only one writing beam leads to the recording of only two rings, which can be placed to the right or left side from the probe beam depending on on the incidence angle.

Similar rings were described in lithium niobate[12] and in poly(methyl methacrylate).[11] The following explanation of this phenomenon was done in Ref. 13. Each medium causes scattering of propagating light. Therefore, even for single beams propagating in the photosensitive medium, one can observe an interference pattern produced by matching the original and scattered beams. In this case, the probe beam used for hologram reading should be scattered two times. The first is regular scattering by the medium, and the second is scattering produced by a hologram of scattered light recorded together with the main hologram. This hologram can be completely reconstructed only by the reading beam of the same wavelength and direction as the writing beam. In the case of different wavelengths or directions of writing and reading beams, the whole hologram of scattered light cannot be read because its wave fronts are not planar.[13] At each angle of incidence the reading beam can read only that part of hologram for which Bragg conditions are satisfied. Because the angular diagram of scattering has cylindrical symmetry, this part should be a ring.

In accordance with this model described in Ref. 13, we can see in Figs. 3(b) and 3(c) diffraction of the reading beam of a He–Ne laser by parts of a hologram of scattered writing UV radiation. We believe that this is original scattering of UV radiation by virgin glass because no increase of scattering was detected in the process of the sample exposure to UV radiation. It was observed in this research that visibility of these rings increases in overdeveloped samples. This process occurs because a refractive-index change in the main hologram saturates whereas the refractive-index change of an underexposed hologram of rings continues to increase (see Subsection 3.D). A fine structure was found inside some of rings [Fig. 3(c), small right ring]. Thus the model in Ref. 13 describes the main features of the discussed phenomenon but some details (complete number and the fine structure of rings) require profound theory to be developed.

D. Properties of Bragg Gratings

Diffraction efficiency of Bragg gratings recorded in PTR glasses was studied as a function of conditions of writing (exposure and spatial frequency of interference pattern) and development (period). An example of the dependence of absolute diffraction efficiency on the thermal treatment period is shown in Fig. 4(a) for one of the PTR specimens. The specimen exposed for 400 mJ/cm^2 underwent consecutive thermal treatments for 10–15 min each at 520 °C, and in intervals between treatments was cooled down to room temperature for diffractive efficiency measurements. The absolute diffraction efficiency was calculated with Eq. (2). Dependence of diffraction efficiency versus development time has an inflection point at the beginning of the process and is saturated at the level of 85% after long heat treatment times. It should be noted that this multiple heat treatment is not the same as a regular development for one or several hours because this procedure includes multiple heating and cooling. However, the curve in Fig. 4(a) shows a tendency of diffraction efficiency to approach a high value after some exposure at elevated temperatures.

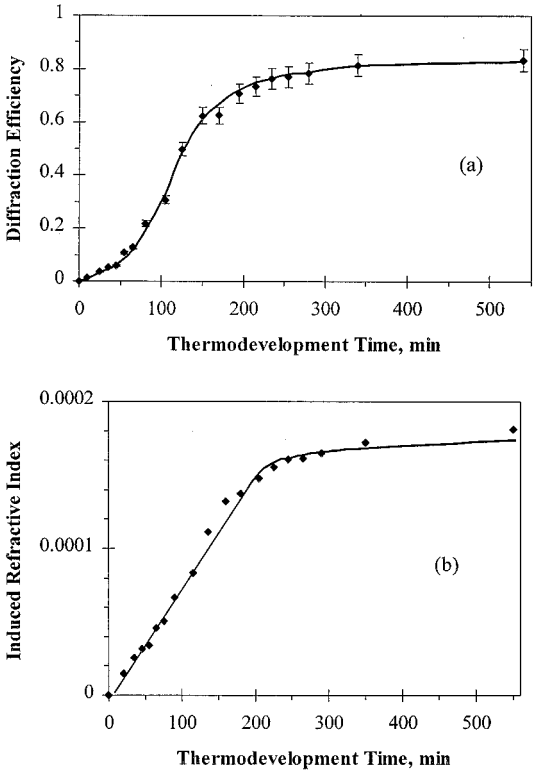

Fig. 4. Effect of the period of thermal treatment on optical properties of diffractive grating in PTR glass: (a) absolute diffraction efficiency and (b) induced refractive index. Exposure was 400 mJ/cm^2 at 325 nm, spatial frequency was 600 mm^{-1}, development was at 520 °C, and specimen thickness was 1.42 mm.

Diffraction efficiency growth at an increasing period of thermal development is obviously caused by refractive-index changes as a result of crystalline phase precipitation.[4–6] Figure 4(b) shows a dependence of a refractive index on the thermal treatment period. This photothermo-induced refractive index was calculated with Kogelnik's Eq. (2) for the sample shown in Fig. 4(a). A linear dependence of an induced refractive index on the thermal treatment period is present in Fig. 4(b). The function $\delta n(t)$ shows no inflection point in comparison with $DE(t)$. A linear dependence $\delta n(t)$ up to the value of 0.00015 allows

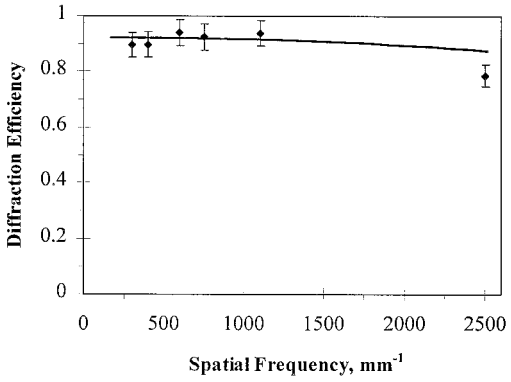

Fig. 5. Dependence of absolute diffraction efficiency on the spatial frequency of the grating. Exposure is 600 mJ/cm^2 at 325 nm and development is 90 min at 520 °C. Specimen thickness is 1.65 mm.

the writing of high-efficiency holograms in glass plates with a thickness more than several hundreds of micrometers.[1] Optical quality of inorganic glass allows use of plates with a thickness up to several centimeters.

Saturation of diffraction efficiency in Fig. 4(a) corresponds to a refractive-index saturation at approximately 0.00017 in Fig. 4(b). No oscillations of diffraction efficiency were recorded in this experiment at a long development period up to 13 h. This means that no significant exceeding of $\pi/2$ for an induced phase was obtained and, consequently, no additional refractive-index growth occurred. The ultimate refractive-index change in similar PTR glass was found at approximately 0.0004 in Ref. 4. This difference between data obtained in Ref. 4 and in this paper can be explained in two ways. The first is that the possible difference in raw materials and glass-melting technology causes a difference in the crystalline-phase precipitation process and ultimately a refractive-index change. The second is a supposition that the recorded saturation of the refractive index in Fig. 4(b) calculated by Eq. (2) could be only a variable part of the total refractive-index change. This means that some steady-state refractive-index change in the exposed area can be caused by the presence of background in an interference pattern or by diffusion of components at distances more than the spatial period of grating in the development process.

The effect of spatial frequency of the interference pattern on diffraction efficiency of the grating in PTR glasses is shown in Fig. 5. This measurement was performed in a thin sample of 1.65 mm in a transmittance configuration when the writing (325 nm) and reading (633 nm) beams were directed from the same side of the glass plate. This configuration allows spatial frequency variations below 2500 mm^{-1}. No optimization was made for exposure or development of gratings with different spatial frequencies. No significant dependence of diffraction efficiency on spatial frequency can be observed in the region from 300 to 2500 mm^{-1} in Fig. 5. The absence of a drop in frequency response at low frequencies is a feature of the PTR process, which requires transport of species in a glass matrix to build the single crystals (tens of nanometers) and does not require transport of species between exposed and unexposed areas. The absence of a drop at high spatial frequencies means that no fringe smearing occurs in the developed interferogram, and consequently no detectable diffusion of components at distances comparable with the half-period of the studied gratings (up to 200 nm) occurs in PTR glass during thermal processing. These data show that diffusion of glass components in the development process cannot affect the saturation in Fig. 4(b), which was observed for grating with a spatial period of 1.6 μm. The study of diffraction efficiency at higher frequencies requires the modification of the experimental setup and will be performed in future research. However, the data shown allow application of Bragg PTR gratings for transmitting elements in all spectral regions and reflecting elements in the IR and visible regions up to 600 nm. The lack of a drop in the amplitude frequency response at low frequencies (Fig. 5) is an advantage of PTR glasses in comparison with photorefractive crystals, which results in a distinct opportunity to design holographic optical elements with small diffraction angles.

An interesting consequence of the low level of induced losses [Fig. 1(c), curve 2] is the rather low sensitivity of PTR grating diffraction efficiency on exposure because underexposure can be compensated by overdevelopment and vice versa. Figure 6 illustrates this feature of PTR glass. In this figure the best diffraction efficiencies for specimens of different thickness from different melts, which underwent different development procedures, are plotted versus exposure to radiation of the He–Cd laser. High absolute diffraction efficiency of 80% and higher is observed in Fig. 6 for exposures ranging between 50 mJ/cm^2 and 5 J/cm^2. Finally, PTR glasses exhibit photosensitivity comparable with the best organic and inorganic materials[1] and allow wide variations of exposure because of image amplification in the process of thermal development.

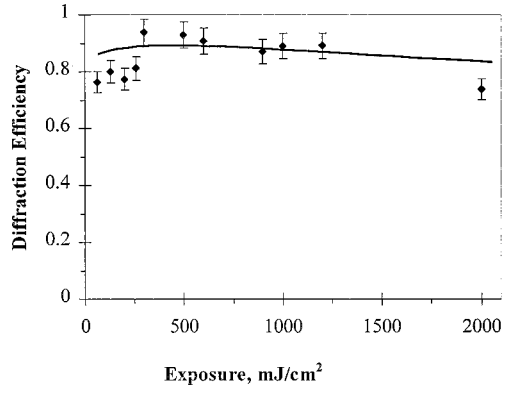

Fig. 6. Maximum absolute diffraction efficiencies of Bragg gratings in PTR glasses that underwent different exposures to radiation of the He–Cd laser at 325 nm.

Some preliminary tests of durability of holograms in PTR glasses have been made. It was found that secondary heat treatment up to 400 °C does not reduce diffraction efficiency. We exposed developed holograms to radiation of a 20-mW He–Ne laser at 633 nm and a 1-mW He–Cd laser at 325 nm for 5–8 h. No hologram destruction was recorded.

4. Conclusions

- PTR glasses (Na_2O-ZnO-Al_2O_3-SiO_2 glass doped with F, Br, Ag, and Ce) are transparent ($A < 1\ cm^{-1}$) from 350 to 4100 nm. Induced losses are approximately 0.1 cm^{-1} in the visible and approximately 0.01 cm^{-1} in the IR region.
- All defects of glass volume (bubbles, stones, etc.), specimen surface (pits, scratches, etc.), and writing beam quality (diffraction on different objects, multiple reflections, etc.) result in the formation of parasitic phase patterns in the recorded area. Scattered writing radiation is recorded as a hologram, which causes parasitic diffractive patterns.
- Absolute diffraction efficiency up to 93% was achieved in PTR glasses of 1–3-mm thickness for grating spatial frequencies up to 2500 mm^{-1} after exposures of 50–500 mJ/cm^2 of He–Cd laser radiation at 325 nm and development at 520 °C.
- Gratings are stable at temperatures up to 400 °C and are not sensitive to the IR, visible, and UV radiation.

This research was supported by Ballistic Missile Defense Organization contract 66001-97-C60008.

References

1. P. Hariharan, "Practical recording materials," in *Optical Holography, Principles, Techniques, and Applications* (Cambridge U. Press, Cambridge, UK, 1996), Chap. 7, pp. 95–124.
2. V. A. Borgman, L. B. Glebov, N. V. Nikonorov, G. T. Petrovskii, V. V. Savvin, and A. D. Tsvetkov, "Photo-thermal refractive effect in silicate glasses," Sov. Phys. Dokl. **34,** 1011–1013 (1989).
3. L. B. Glebov, N. V. Nikonorov, E. I. Panysheva, G. T. Petrovskii, V. V. Savvin, I. V. Tunimanova, and V. A. Tsekhomskii, "Polychromatic glasses—a new material for recording volume phase holograms," Sov. Phys. Dokl. **35,** 878–880 (1990).
4. L. B. Glebov, N. V. Nikonorov, E. I. Panysheva, G. T. Petrovskii, V. V. Savvin, I. V. Tunimanova, and V. A. Tsekhomskii, "New ways to use photosensitive glasses for recording volume phase holograms," Opt. Spectrosc. **73,** 237–241 (1992).
5. S. D. Stookey, "Photosensitive glass (a new photographic medium)," Ind. Eng. Chem. **41,** 856–861 (1949).
6. S. D. Stookey, G. H. Beall, and J. E. Pierson, "Full-color photosensitive glass," J. Appl. Phys. **49,** 5114–5123 (1978).
7. N. F. Borrelli, J. B. Chodak, D. A. Nolan, and T. P. Seward, "Interpretation of induced color in polychromatic glasses," J. Opt. Soc. Am. **69,** 1514–1519 (1979).
8. A. V. Dotsenko, A. M. Efremov, V. K. Zakharov, E. I. Panysheva, and I. V. Tunimanova, "Absorption spectra of multichromatic glasses," Sov. J. Glass Phys. Chem. **11,** 592–595 (1985).
9. L. Levy, "Applied optics," in *Physical Optics: The Wave Nature of Light* (Wiley, New York, 1968), Chap. 2, pp. 35–123.
10. E. N. Boulos and N. J. Kreidl, "Water in glass: a review," J. Can. Ceram. Soc. **41,** 83–86 (1972).
11. M. Moran and I. P. Kaminow, "Properties of holographic grating photoinduced in polymethyl methacrylate," Appl. Opt. **12,** 1964–1970 (1973).
12. M. R. B. Forshaw, "Explanation of two-ring diffraction phenomenon observed by Moran and Kaminow," Appl. Opt. **13,** 2 (1974).
13. R. Magnusson and T. K. Gaylor, "Laser scattering induced holograms in lithium niobate," Appl. Opt. **13,** 1545–1548 (1974).